Macromolecules

ARTICLE

pubs.acs.org/Macromolecules

Disorder-to-Order Transition of Triblock Comb Copolymer $A_{m+1}(BC)_m$

Zhiyuan Qian and Rong Wang*

Department of Polymer Science and Engineering, State Key Laboratory of Coordination Chemistry, School of Chemistry and Chemical Engineering, National Laboratory of Microstructures, Nanjing University, Nanjing 210093, China

ABSTRACT: The disorder to order transition of comb copolymer $A_{m+1}(BC)_m$ is investigated by the self-consistent field theory. The interaction parameters between the three different blocks are considered by varying the composition of the comb triblock copolymer with the side chain number $m = 1$ and 3. As the side chain number m increases, the Flory–Huggins interaction parameter of disorder to order transition (DOT) increases and the lowest DOT occurs when the volume fractions of blocks A, B, and C are approximately equal. When one component is the minority, the disorder-to-order transition curve is similar to binary $A_{m+1}B_m$ comb copolymer. The influence of the side chain density on phase transition is also discussed. The comb copolymer is more difficult to phase separate with larger side chain number m and shorter side chain.

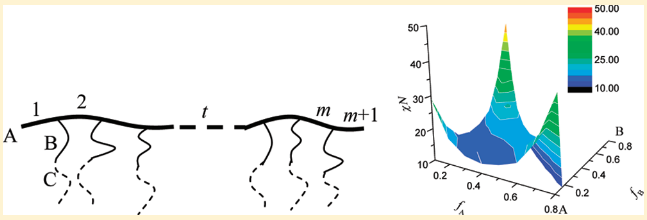

1. INTRODUCTION

Block copolymers can microphase separate to form a variety of ordered nanoscale morphologies.[1,2] This unique characteristic of block copolymers provides possibilities for their potential applications in nanoscience, such as molecular actuators,[3] nanotubes,[4] and other carbon nanostructures.[5] Therefore, block copolymers have attracted a great deal of attention both in theory and experiment. Comb copolymers can be composed of a long, flexible or stiff, hydrophobic backbone and dense, long or short, hydrophilic side chains that branch from this main chain. By changing these chain sections, properties such as phase behavior,[6] morphology,[7] and order to disorder transitions[8] can be modified. With the improvement in synthetic techniques, graft block copolymers with well-defined molecular architectures have been formulated successfully.[9,10] Xia and co-workers[11] have recently synthesized narrowly dispersed brush block copolymers (*g*-[PLA_x-*b*-P*n*BA_y]) and random copolymers (*g*-[PLA_x-*ran*-P*n*BA_y]). They found that the side chains of brush random copolymers containing approximately equal volume fractions of PLA and P*n*BA can microphase separate into lamellar morphology with domain spacing of about 14 nm, and the domain spacing and T_{DOT} were insensitive to the brush copolymer backbone length, while the brush block copolymers with the same number of PLA and P*n*BA self-assembles into highly ordered lamellae with domain spacing over 100 nm. Liu and co-workers[12] successfully synthesized hyperbranched polyethylenimine grafted polycaprolactone block monomethoxyl poly(ethylene glycol) copolymers (hy-PEI-*g*-PCL-*b*-mPEG) and found that the application in DNA delivery studies displayed a strong effect of PCL and mPEG chain lengths and graft density on cytotoxicity, and longer mPEG chains, longer PCL segments and higher graft densities led to lower cytotoxicity.

In recent years, the comb copolymer $A_{m+1}(BC)_m$ was experimentally studied.[10,13] The brush copolymers poly(2-hydroxyethylmathacrylate)-*graft*-poly(ε-caprolactone)-*block*-poly(ethylene oxide) (PHEMA-*g*-(PCL-*b*-PEO)) have double crystallizable side chains.[10] For brush copolymer, the melt temperature (T_m) and degree of crystallinity (X_c) values of PCL block decrease with the increase of chain length of PEO block. The crystallization temperature (T_c), T_m and X_c of poly(2-hydroxyethylmathacrylate)-*graft*-poly(ε-caprolactone) (PHEMA-*g*-PCL) were enhanced with the chain length increase of poly(ε-caprolactone) (PCL). The graft polymer PVAc-*g*-[P(AN-*r*-BVE)-*b*-PCHO] was synthesized in "one-step" by radical/cationic transformation polymerization and coupling reaction.[13] In the case of PVAc-*g*-[P(AN-*r*-BVE)-*b*-PCHO], the two glass transition temperature (T_{g1}, T_{g2}) were 26 and 43 °C, respectively. It is likely that T_{g1} and T_{g2} correspond to glass transitions for the P(AN-*r*-BVE)-*b*-PCHO grafts (34 °C) and the PVAc backbone (39 °C), respectively. T_{g1} is slightly lower than T_g for P(AN-*r*-BVE)-*b*-PCHO because propagation of PCHO was disturbed by the coupling reaction with PVAc–OH and average molar mass of P(AN-*r*-BVE)-*b*-PCHO grafts was lower than that for P(AN-*r*-BVE)-*b*-PCHO obtained in the absence of PVAc–OH. T_{g2} is slightly higher than T_g for PVAc–OH, indicating that the movement of PVAc backbone is somehow restricted by the P(AN-*r*-BVE)-*b*-PCHO grafts. Therefore, it is very important to study phase transition of the comb copolymer $A_{m+1}(BC)_m$ with complex architectures. Moreover, there are many studies related to disorder to order transition (DOT) of block copolymers, such as alkyne/azide click chemistry induced DOT of diblock copolymer.[14] Even some new techniques are developed to probe the disorder to order transition, such as positron annihilation lifetime spectroscopy.[15]

We have already studied the morphology of comb copolymer $A_{m+1}(BC)_m$ in our previous work.[16] In that work, we found the disordered phase exists at the corner of the phase diagram besides the ordered morphologies. The disordered phase easily exists at the corner of block B or block A. The block B or block A is completely or partly restricted. In fact, we

Received: March 15, 2011
Revised: July 3, 2011
Published: July 18, 2011

dx.doi.org/10.1021/ma200572h | *Macromolecules* 2011, 44, 6113–6120

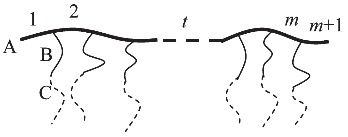

Figure 1. Schematic representation of a comb copolymer molecule. Thick line, thin solid, and thin dash lines represent main chain A and side blocks B and C, respectively.

want to know the essence of the difference at the three different corners and the extent of the influence of the interaction parameters on the phase behavior of this complex block copolymer.

In recent years, SCFT method has been largely used to study the phase behavior of block copolymers. It is also used to study the disorder to order transition of block copolymers.[17,18] Even the SCFT method has been used to successfully study the polydispersity induced disorder to order transition of block copolymers.[19−22] Therefore, we consider the disorder to order transition of comb copolymer $A_{m+1}(BC)_m$ with different side chain numbers by using the self-consistent field theory (SCFT) in this study. Because of the complexity of this comb copolymer $A_{m+1}(BC)_m$, we only consider the stability of the homogeneous phase relative to the microseparated state. The related parameters are the side chain number m, the volume fraction of blocks A, B, and C and the Flory−Huggins parameter χN. We construct the phase diagram of disorder to order transition of comb copolymer $A_{m+1}(BC)_m$ by continuously varying the composition of the block copolymer. And the side chain number is also considered in this work.

2. CALCULATION ALGORITHM

We consider n comb copolymer $A_{m+1}(BC)_m$ with polymerization N in a volume V and there are m branching points (or the side chain number) along the main chain A, which divide the main chain as $m + 1$ equal parts (we called it "divided sections") with polymerization N_A and each side chain BC has N_B and N_C segments for blocks B and C, respectively. So, $N = (m + 1)N_A + m(N_B + N_C)$. The schematic diagram of a comb copolymer molecule is presented in Figure 1. The monomers of the main chain and the side ones are assumed to be flexible with a statistical length a. Therefore, the compositions (average volume fractions) are $f_A = (m + 1)N_A/N, f_B = mN_B/N, f_C = 1 - f_A - f_B$ for the main chain A and the blocks B and C of the side chains BC, respectively.

With the different architectures of the blocks A, B and C, we define four distribution functions, i.e., $q_{BC}(\mathbf{r}, s)$, $q_{BC}^+(\mathbf{r}, s, t)$, $q_A(\mathbf{r}, s, t)$, and $q_A^+(\mathbf{r}, s, t)$, where s is the contour along the main chain for A and along the side chain for BC, t is the number along the main chain A divided by the side chains BC and it belongs to $[1, m + 1]$. With these definitions, the polymer segment probability distributions q and q^+ for main chain A and side chain BC satisfy the modified diffusion equations:

$$\frac{\partial}{\partial s} q = \frac{Na^2}{6} \nabla^2 q - wq \tag{1}$$

$$\frac{\partial}{\partial s} q^+ = -\frac{Na^2}{6} \nabla^2 q^+ + wq^+ \tag{2}$$

where w is w_A when s belongs to block A, w_B when belongs to block B, and w_C when belongs to block C. The initial conditions are $q_{BC}(\mathbf{r}, 0) = 1$, $q_A(\mathbf{r}, 0, 1) = 1$, $q_A(\mathbf{r}, 0, t + 1) = q_{BC}(\mathbf{r}, N_B + N_C)q_A(\mathbf{r}, N_A, t)$, $q_A^+(\mathbf{r}, N_A, m + 1) = 1$, $q_A^+(\mathbf{r}, N_A, t) = q_A^+(\mathbf{r}, 0, t + 1)q_{BC}(\mathbf{r}, N_B + N_C)$ and $q_B^+(\mathbf{r}, N_B + N_C, t) = q_A(\mathbf{r}, N_A, t)\, q_A^+(\mathbf{r}, 0, t + 1)$, where $t \in [1, m]$. Accordingly, the partition function of a single chain subject to the mean field w_i, where i represents block species A, B, and C, can be written as $Q = \int d\mathbf{r}\, q_A(\mathbf{r}, N_A, m + 1)$.

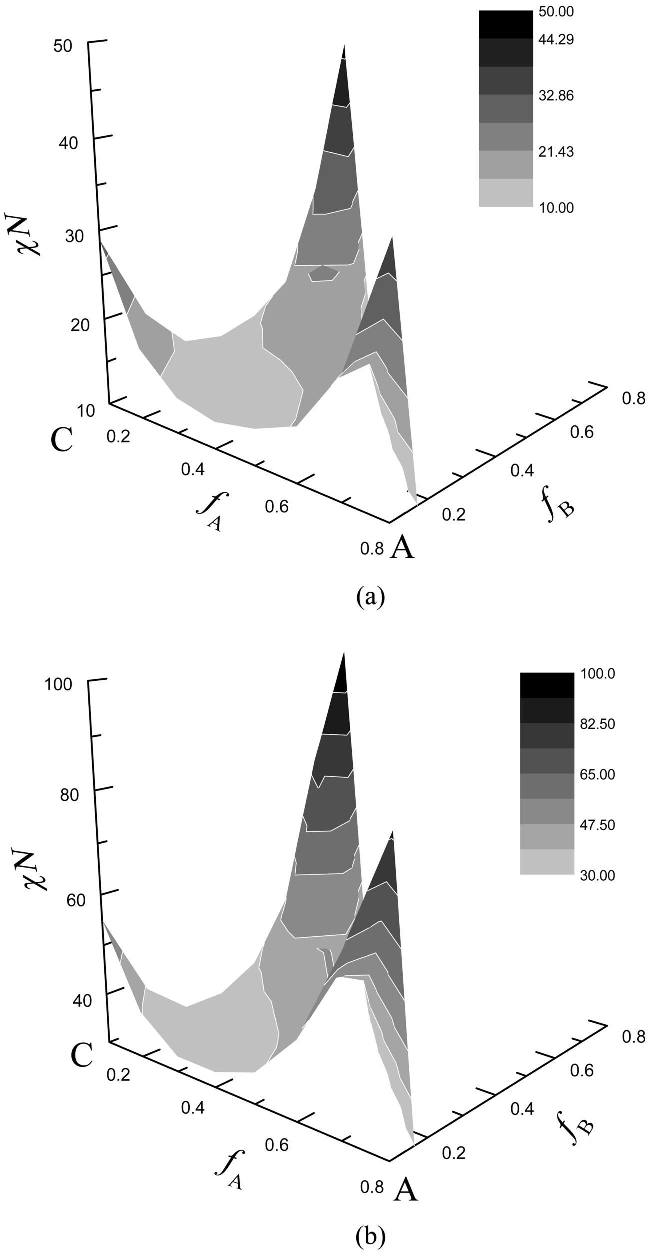

Figure 2. Phase diagram for triblock comb copolymer $A_{m+1}(BC)_m$ with different side chain number m: (a) $m = 1$; (b) $m = 3$.

With above description, the free energy function (in units of k_BT) of the system is given by

$$F = -\ln(Q/V) + 1/V \int d\mathbf{r}\, \Big[\sum_{i \neq j} \chi_{ij} N \phi_i \phi_j - \sum_i w_i \phi_i - \xi\big(1 - \sum_i \phi_i\big)\Big] \tag{3}$$

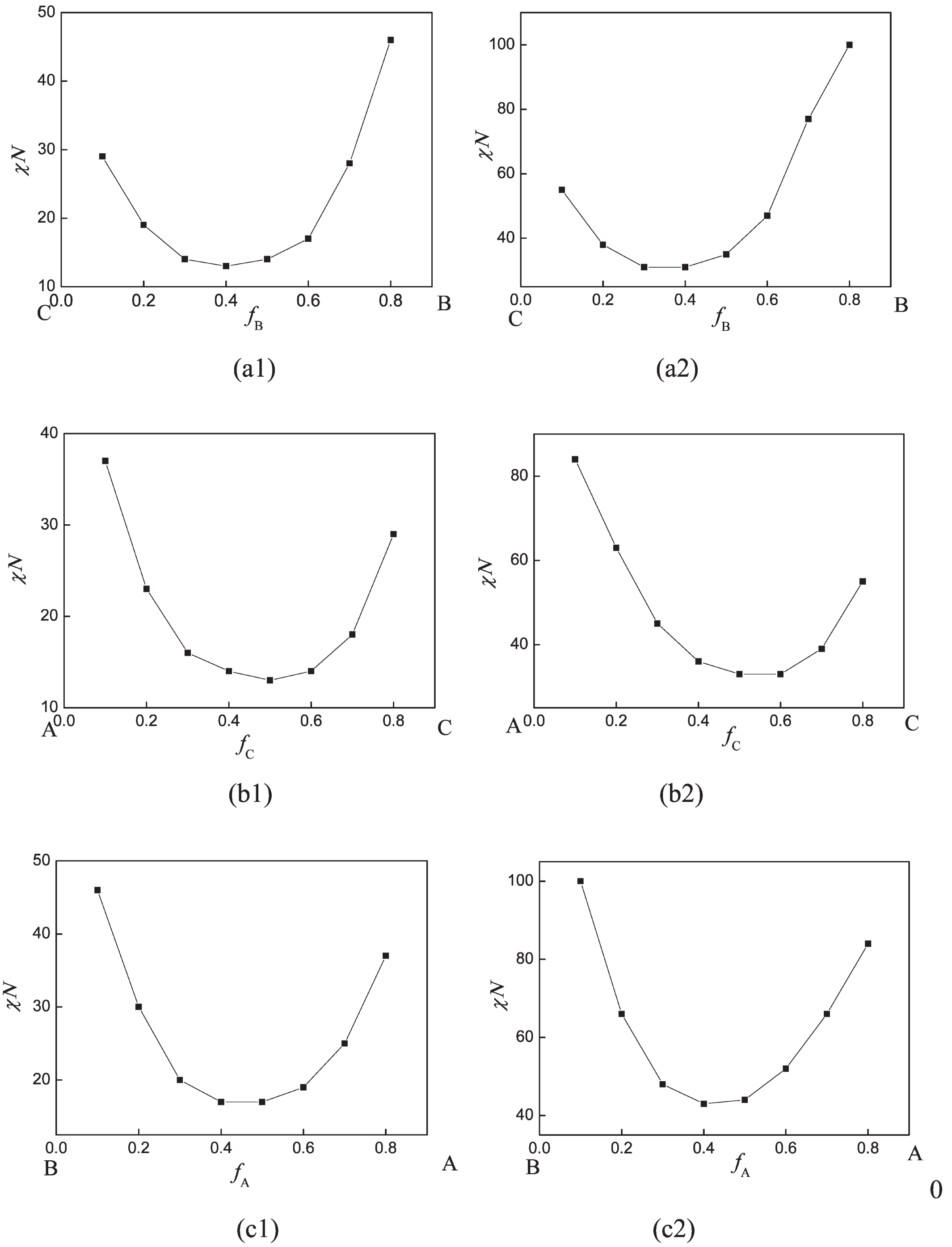

Figure 3. Phase diagram for triblock comb copolymer $A_{m+1}(BC)_m$ with the volume fraction of one block is small. Left figures are for $m = 1$ and right ones for $m = 3$. Key: (a1) $m = 1, f_A = 0.1$; (a2) $m = 3, f_A = 0.1$; (b1) $m = 1, f_B = 0.1$; (b2) $m = 3, f_B = 0.1$; (c) $m = 1, f_C = 0.1$; (c2) $m = 3, f_C = 0.1$.

where χ_{ij} is the Flory–Huggins interaction parameter between different species ($i, j = A, B, C, i \neq j$), ϕ_i is the monomer density of each species ($i = A, B, C$), and ξ is the Lagrange multiplier (as a pressure).

Minimization of the free energy to mean field, density and pressure, $\delta F/\delta w = \delta F/\delta \phi = \delta F/\delta \xi = 0$, leads to the following self-consistent field equations that describe the equilibrium state:

$$\phi_A(\mathbf{r}) = \frac{V}{QN}\sum_{t=1}^{m+1}\int_0^{N_A} ds\, q_A(\mathbf{r}, s, t) q_A^{+}(\mathbf{r}, s, t) \qquad (4)$$

$$\phi_B(\mathbf{r}) = \frac{V}{QN}\sum_{t=1}^{m}\int_{N_C}^{N_B + N_C} ds\, q_{BC}(\mathbf{r}, s) q_{BC}^{+}(\mathbf{r}, s, t) \qquad (5)$$

$$\phi_C(\mathbf{r}) = \frac{V}{QN}\sum_{t=1}^{m}\int_0^{N_C} ds\, q_{BC}(\mathbf{r}, s) q_{BC}^{+}(\mathbf{r}, s, t) \qquad (6)$$

$$w_A(\mathbf{r}) = \chi_{AB}N\phi_B(\mathbf{r}) + \chi_{AC}N\phi_C(\mathbf{r}) + \xi(\mathbf{r}) \qquad (7)$$

$$w_B(\mathbf{r}) = \chi_{AB}N\phi_A(\mathbf{r}) + \chi_{BC}N\phi_C(\mathbf{r}) + \xi(\mathbf{r}) \qquad (8)$$

$$w_C(\mathbf{r}) = \chi_{AC}N\phi_A(\mathbf{r}) + \chi_{BC}N\phi_B(\mathbf{r}) + \xi(\mathbf{r}) \tag{9}$$

$$\phi_A(\mathbf{r}) + \phi_B(\mathbf{r}) + \phi_C(\mathbf{r}) = 1 \tag{10}$$

Here we solve eqs 4−10 directly in real space by using a combinatorial screening algorithm proposed by Drolet and Fredrickson.[23,24] Note that one must solve the diffusion equation first for $q_{BC}(\mathbf{r}, s)$ with initial condition $q_{BC}(\mathbf{r}, 0) = 1$, then for $q_A(\mathbf{r}, s, t)$ with $q_A(\mathbf{r}, 0, 1) = 1$, $q_A(\mathbf{r}, 0, t + 1) = q_{BC}(\mathbf{r}, N_B + N_C)q_A(\mathbf{r}, N_A, t)$, for $q_A^+(\mathbf{r}, s, t)$ with $q_A^+(\mathbf{r}, N_A, m + 1) = 1$, $q_A^+(\mathbf{r}, N_A, t) = q_A^+(\mathbf{r}, 0, t + 1)q_{BC}(\mathbf{r}, N_B + N_C)$ and last for $q_{BC}^+(\mathbf{r}, s, t)$ with $q_{BC}^+(\mathbf{r}, N_B + N_C, t) = q_A(\mathbf{r}, N_A, t)\, q_A^+(\mathbf{r}, 0, t + 1)$. Each iteration continues until the phase is stable and the free energy converges to 10^{-6}. Several times are repeated by using different initial conditions to avoid the trapping in a metastable state. In addition, we also minimize the free energy with respect to the system size because it has been pointed out that the box size is an important factor.[25] The implementation of the self-consistent field theory is carried out in a three-dimensional $L_x \times L_y \times L_z$ lattice with periodic boundary conditions.

Because of the complexity of this comb block copolymer $A_{m+1}(BC)_m$, we only consider three cases to explore the disorder to order phase transition interaction parameters: (1) $A_{m+1}(BC)_m$ (m = 1 and 3) with identical interaction parameters, (2) $A_{m+1}(BC)_m$ (m = 1 and 3) when the interaction between the blocks A and C are fixed, (3) side chain number effect (m changes from 1 to 5). Thus, we calculate the crossover curve of the disordered phase and an (unspecified) ordered phase in terms of the normalized Flory−Huggins parameter χN, the relative composition, and the number of teeth in the comb m.

By systematically changing the volume fractions of the A, B, and C blocks, we can construct the component phase diagrams in the entire range of the copolymer composition.

3. RESULTS AND DISCUSSION

3.1. Phase Diagrams for $A_{m+1}(BC)_m$ (m = 1 and 3) with Identical Interaction Parameters $\chi_{AB}N = \chi_{AC}N = \chi_{BC}N = \chi N$. By changing the volume fractions of the three different blocks (f_A, f_B and f_C) and the Flory−Huggins parameter χN, we obtained the phase diagrams of the triblock copolymer with side chain number m. Only the cases for the side chain number m = 1 and 3 are considered in this part. The interaction parameters between different blocks are set to be equal:$\chi_{AB}N = \chi_{AC}N = \chi_{BC}N = \chi N$. The chain length is N = 60 and 120 for m = 1 and 3, respectively. The phase diagram for triblock copolymer with side chain number m = 1, 3 are shown in Figure 2, parts a and b, respectively. From the figure, we can see that the disorder to order transition parameter χN is larger at the corners of the three blocks. This point can confirm our previous results, where the disordered phase is stable when the block B or block A is the majority.[16] The χN of the disorder to order transition (DOT) is low when the volume fractions of the three blocks are comparable. With the side chain number m increasing, the χN of the disorder to order transition increases largely, which corresponds to the lower temperature to microphase separate, i.e., the system becomes more stable. We can see that the χN of the disorder to order transition is larger when the triblock copolymer has the longer main chain A or longer side chain with short block C, i.e., longer block A or longer block B, and it is easier for the copolymer to transform from disordered phase to ordered phase when the volume fractions (f_A, f_B, and f_C) of different blocks are approximately equal.

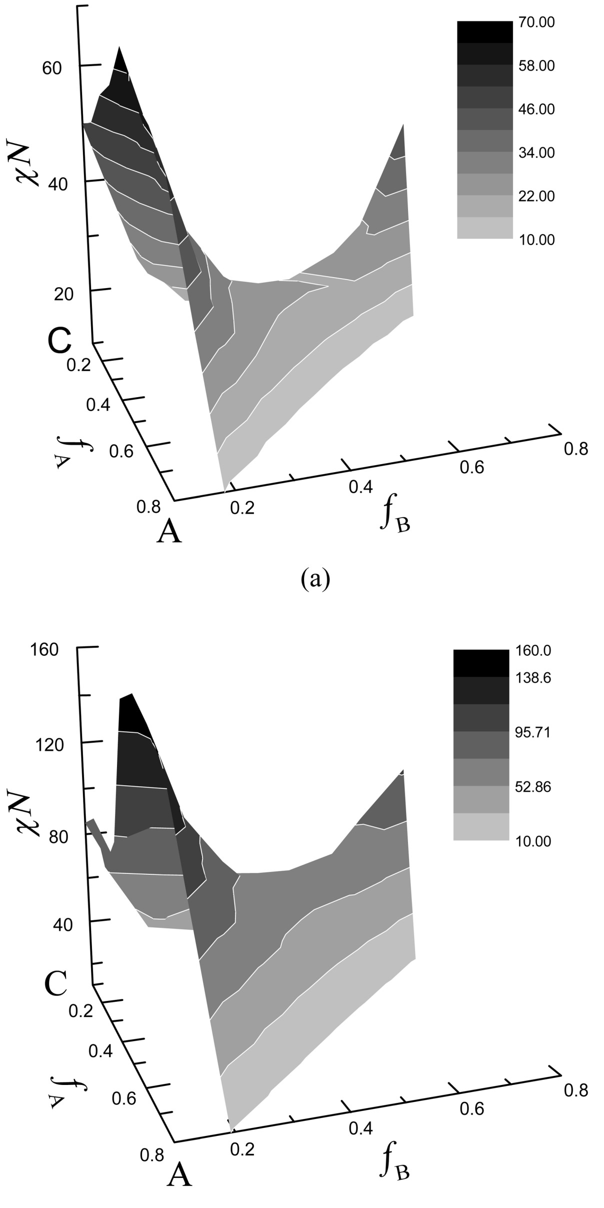

(a)

(b)

Figure 4. Phase diagram for triblock comb copolymer $A_{m+1}(BC)_m$ with different side chain number and different interaction parameter between block A and C. Key: (a) m = 1, $\chi_{AC}N$ = 10; (b) m = 3, $\chi_{AC}N$ = 30.

In order to compare the difference of the phase diagrams between diblock comb copolymer $A_{m+1}B_m$ and triblock comb copolymer $A_{m+1}(BC)_m$, we also give the phase diagrams when the volume fractions f_A, f_B, f_C = 0.1, respectively, which are shown in Figure 3. From the phase diagrams, we can see that when the volume fraction f_A, f_B, or f_C is small, the diagrams are similar to those of diblock comb copolymer, and the minimum of χN is in agreement with the binary comb block copolymer. When f_A is small, it is harder for the copolymer to transform from disordered phase to ordered phase while f_B is large, due to the segments of block B are restricted by block A and C. When f_B is small, the sections of block A are confined by blocks B and C, so the

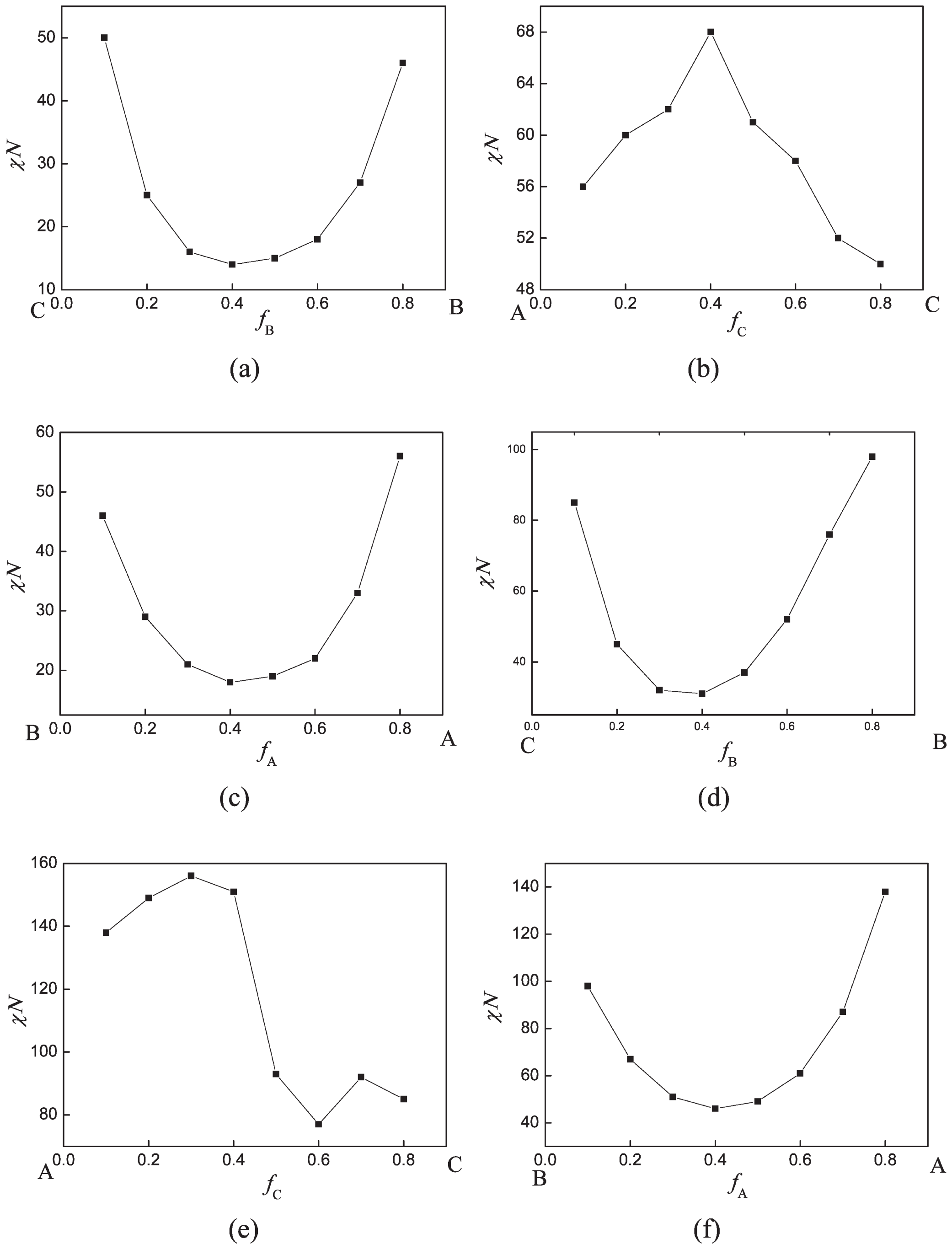

Figure 5. Phase diagram for triblock comb copolymer $A_{m+1}(BC)_m$ with the volume fraction of one block is small. Key: (a) $m = 1, \chi_{AC}N = 10, f_A = 0.1$; (b) $m = 1, \chi_{AC}N = 10, f_B = 0.1$; (c) $m = 1, \chi_{AC}N = 10, f_C = 0.1$; (d) $m = 3, \chi_{AC}N = 30, f_A = 0.1$; (e) $m = 3, \chi_{AC}N = 30, f_B = 0.1$; (f) $m = 3, \chi_{AC}N = 30, f_C = 0.1$.

$\chi_{(DOT)}N$ is large while f_A is large. When f_C is small, both the sections of block A and B are restricted, the $\chi_{(DOT)}N$ is large while the A or B is the majority. However, due to the restricted segments of block B are more than that of block A, the influence of block B on the disorder to order transition is larger than that of block A, which means the $\chi_{(DOT)}N$ is larger when f_B is large. From the above analysis, we can obtain the phase separation sequence: first block C, then block A and the last block B, which is decided by the architecture of the block copolymer. It is in agreement with our previous work, where the results show that the block C easily phase separates, then the block A and the last the block B.[16] Comparing the phase diagrams when side chain number $m = 1$ with $m = 3$, we can see the χN with the side chain number $m = 3$ is approximately triple the χN with the side chain number $m = 1$ when the volume fractions of the three or two blocks are equal. This phenomena is also observed in $A_{m+1}B_m$ diblock comb copolymer.[26] The confined segments increase with side chain number increasing, so the χN increases, which means lower temperatures to microphase separate.

3.2. Phase Diagram for $A_{m+1}(BC)_m$ with $\chi_{AC}N$ Fixed. We also studied the phase transition behavior of triblock comb copolymer with the asymmetric interaction parameters. Considering the complexity of the copolymer, we set the interaction parameter between the blocks A and C is fixed, and the rest interaction parameters are equal: $\chi_{AB}N = \chi_{BC}N = \chi N$. We set $\chi_{AC}N = 10$ for $m = 1$ and $\chi_{AC}N = 30$ for $m = 3$. Here, $\chi_{AC}N = 30$ for $m = 3$ is for simple consideration.[26−29] The phase diagrams are shown in Figure 4a,b. From the diagrams, we can get similar conclusions with 3.1. But the χN of the disorder to order transition is larger than the corresponding χN with equal interaction parameters. This is due to the fact that we set the relatively small interaction between the blocks A and C ($\chi_{AC}N = 10$ for $m = 1$ and $\chi_{AC}N = 30$ for $m = 3$). This means that it is a little frustrated, $\chi_{AB}N = \chi_{BC}N = \chi N > \chi_{AC}N$. Therefore, the disorder to order transition is more complex. As the side chain number m increases, the χN of the disorder to order transition increases greatly, which means a lower temperature to microphase separation; i.e., the system becomes more stable with larger side chain number. The χN of the disorder to order transition is larger when the comb copolymer has the longer main chain A or longer side chain with short block C, i.e., longer block A or longer block B and it is easier for the copolymer to transform from disorder phase to order phase when the volume fractions (f_A, f_B, and f_C) of different blocks are approximately equal. Compared with the three corners of the phase diagram, we can see the χN at the corner of block B is lower the other two corners. In this case, we can conclude that the block B can separate from the copolymer first, then the blocks A and C phase separate. But the separation sequence of the blocks A and C is difficult to decide. We can also see the complex phase behavior below. We present the phase diagrams shown in Figure 5a−f when the volume fraction is f_A, f_B, f_C = 0.1, respectively. Figure 5a−c gives the results when $m = 1$, $\chi_{AC}N = 10$. From the figures, we can see that when the volume fraction of block A or C is small, the phase diagrams are similar to the diagrams of diblock copolymer, and the minimum of χN is in agreement with the binary block copolymer. Figure 5d−f shows the results for the case $m = 3$, $\chi_{AC}N = 30$ when the blocks A, B, and C are the minority, respectively. When the volume fractions f_A and f_C are small, the diagrams are similar to the diagrams of diblock copolymer.

However, the phase diagram is different from that of diblock comb copolymer when the volume fraction of block B f_B is small. Even the phase transition curve is complex. This phenomenon is a little strange showing a saddle plane near the edge of the AC. On this condition, the block B has limited contribution to the phase separation and the separation of the blocks A and C is dominant. But the repulsive interaction parameter $\chi_{AC}N$ is a little weak. Therefore, the χN of the disorder to order transition of the block copolymer is very large.

3.3. Influence of the Side Chain Number *m*.

3.3.1. N_A, N_B, and N_C Fixed. From the above results, we can see that the side chain number has great effect on the phase behavior of triblock comb copolymer $A_{m+1}(BC)_m$. In this part, we consider two cases by changing the side chain number: one is the lengths of blocks A, B and C fixed and the other is the main chain length fixed. The interaction parameters between different blocks are set to be equal: $\chi_{AB}N = \chi_{AC}N = \chi_{BC}N = \chi N$. Figure 6a is the disorder to order transition curve with the fixed lengths of side chains and main chain sections as a function of the side chain number m. The interaction parameter χN of the disorder to order transition increases with the side chain number increasing, which means the triblock copolymer becomes more stable. When the side chain length is equal to that of the main chain sections, such as $N_A = 10$, $N_B = N_C = 5$ (spheres), the χN increases linearly with the side chain number m. When the side chain length is longer than the main chain sections, such as $N_A = 5$, $N_B = N_C = 5$ (squares), the χN is smaller than that of the case for $N_A = 10$, $N_B = N_C = 5$ (spheres), which corresponds to the equal lengths between the main section and the side chain. When the main chain section length is longer than the side chain, such as $N_A = 20$, $N_B = N_C = 5$ (triangles), the χN is larger than that of the case for $N_A = 10$, $N_B = N_C = 5$ (spheres). As the main sections (side chain number) increase, the restricted sections increase. It is favorable for the stability of the system, which corresponds to the χN of the disorder to order transition increases.

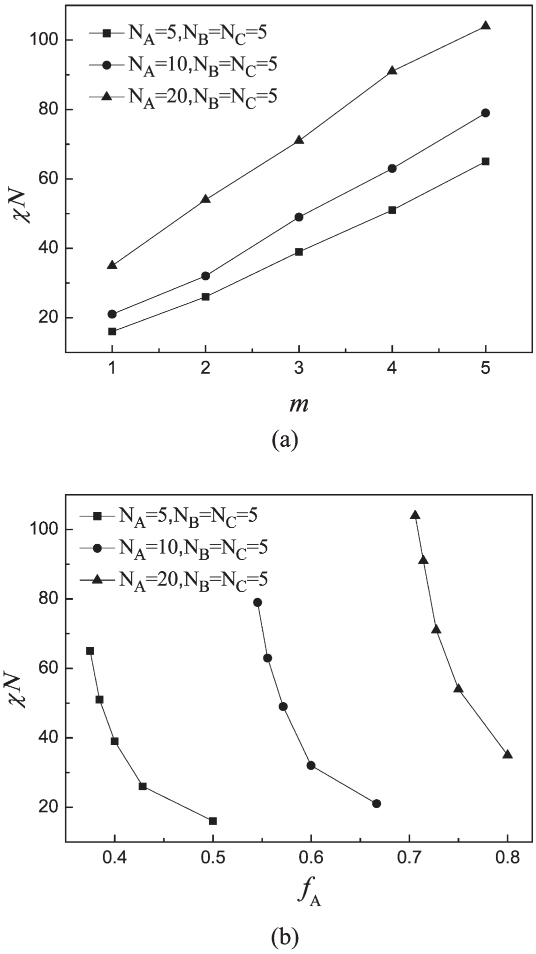

Figure 6. Disorder to order transition curves with the fixed lengths of the blocks (1) $N_A = 5$, $N_B = N_C = 5$ (squares), (2) $N_A = 10$, $N_B = N_C = 5$ (spheres), and (3) $N_A = 20$, $N_B = N_C = 5$ (triangles). Key: (a) χN versus m; (b) χN versus f_A.

Figure 6b is the disorder to order transition curve with the fixed lengths of side chains and the main chain sections as a function of the volume fraction of main chain converted from the side chain number, i.e., $f_A = (m + 1)N_A/((m + 1)N_A + m(N_B + N_C))$. From the graph, we can see that the behavior of the disorder to order transition is similar at different ratios ($\lambda = N_A/(N_B + N_C)$) of the lengths of the main chain section and the side chain. Though the volume fraction of the main chain f_A decreases slower with the side chain number increasing, the χN of the disorder to order transition increases largely. As a result, the curves become sharp when the side chain number is large, especially for $\lambda < 1$. Comparing these curves, we can conclude that the comb

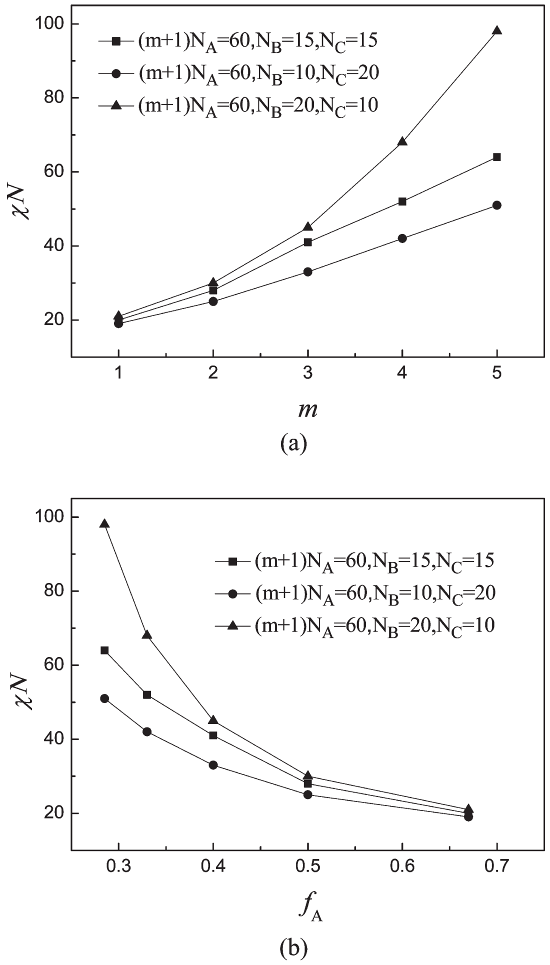

Figure 7. Disorder to order transition curves with the fixed main chain length $(m+1)N_A = 60$ and the side chain length $(N_B + N_C) = 30$ (1) $N_B = 15$, $N_C = 15$ (squares), (2) $N_B = 10$, $N_C = 20$ (spheres), (3) $N_B = 20$, $N_C = 10$ (triangles), where $f_A = (m+1)N_A/((m+1)N_A + m(N_B + N_C))$.

copolymers are more stable with shorter side chain and larger side chain number.

3.3.2. $(m + 1)N_A$, $(N_B + N_C)$ Fixed. There is another case that the side chain number will influence the disorder to order transition behavior. If the main length and the side chain length are fixed, the transition behavior will change largely as the side chain number increases, i.e. the side chain density increases. Figure 7 gives the curves of the disorder to order transition with different side chain number at the fixed main chain length $(m+1)N_A = 60$ and side chain length $(N_B + N_C) = 30$. We considered the cases when the length of block B is equal to that of block C (i.e., $N_B = N_C = 15$), or larger (i.e., $N_B = 20$, $N_C = 10$), or smaller (i.e., $N_B = 10$, $N_C = 20$) than that of block C, respectively. The χN of the disorder to order transition increases with the increasing of volume fraction of block B. As the side chain number increases, the side chain density increases, and the volume fraction of the main chain f_A decreases, while the χN of the disorder to order transition increases. When the side chain number m begins to increase ($m = 1 \rightarrow 3$), the volume fraction of each block does not change significantly compared with the larger side chain number ($m = 3 \rightarrow 5$). Figure 7 shows that the χN of the disorder to order transition increases with the increasing of the side chain number m (or the decreasing of f_A), which confirms that the system is more stable with the increasing of the side chain number (or density).

4. CONCLUSIONS

The disorder to order transition behaviors of triblock copolymer $A_{m+1}(BC)_m$ are successfully studied by the numerical version of the self-consistent field theory. With the increase of side chain number m, the χN of the disorder to order transition increases. When the volume fraction of block is small, the phase diagrams are similar to that of diblock copolymer. Because the blocks A and B are restricted, it is harder for copolymer to transfer from disorder to order as f_A or f_B is larger. The blocks B are more restricted than blocks A, as a result, the influence of block B to disorder to order transition is larger than block A. With the lengths of the main chain sections and the side chains fixed, the $\chi_{(\mathrm{DOT})}N$ increases as the side chain number increases. The copolymer is more stable with shorter side chain and larger side chain number. And the χN of the disorder to order transition increases with the increasing of side chain number as the length of main chain is fixed, corresponds to the system is more stable with the increasing of side chain number (density). When the interaction parameters are not identical, the phase behavior is more complex. Our results are helpful to design materials with complex architecture or tailor the phase behavior of comb copolymers and to understand the phase behavior of these complex block copolymers.

AUTHOR INFORMATION

Corresponding Author

*E-mail: rong_wang73@hotmail.com.

ACKNOWLEDGMENT

We gratefully acknowledge financial support from National Natural Science Foundation of China (Nos. 20874046 and 21074053), National Basic Research Program of China (No. 2010CB923303), and Fundamental Research Funds for the Central Universities (No.1095020515).

REFERENCES

(1) Hamley, I. W. *The physics of Block Copolymers*; Oxford University Press: New York, 1998.

(2) Balsamo, V.; Collins, S.; Hamley, I. W. *Polymer* **2002**, *43*, 4207.

(3) Li, C. M.; Gunari, N.; Fischer, K.; Janshoff, A.; Schmidt, M. *Angew. Chem., Int. Ed.* **2004**, *43*, 1101.

(4) Huang, K.; Rzayev, J. *J. Am. Chem. Soc.* **2009**, *131*, 6880.

(5) Tang, C.; Dufour, B.; Kowalewski, T.; Matyjaszewski, K. *Macromolecules* **2007**, *40*, 6199.

(6) Pugh, C.; Kiste, A. L. *Prog. Polym. Sci.* **1997**, *22*, 601.

(7) Matsushita, Y.; Noda, I.; Torikai, N. *Macromol. Symp.* **1997**, *124*, 121.

(8) Hatada, K.; Kitayama, T. *Polym. Int.* **2000**, *49*, 11.

(9) Jannasch, P.; Loyens, W. *Solid State Ionics* **2004**, *166*, 417.

(10) Yuan, W. Z.; Yuan, J. Y.; Zhang, F. B.; Xie, X. M.; Pan, C. Y. *Macromolecules* **2007**, *40*, 9094.

(11) Xia, Y.; Olsen, B. D.; Kornfield, J. A.; Grubbs, R. H. *J. Am. Chem. Soc.* **2009**, *131*, 18525.

(12) Liu, Y.; Nguyen, J.; Steele, T.; Merkel, O.; Kissel, T. *Polymer* **2009**, *50*, 3895.

(13) Lai, R. F.; Guo, H. Q.; Kamachi, M. *Polymer* **2009**, *50*, 3582.

(14) Wei, X. Y.; Chen, W.; Chen, X. J.; Russell, T. P. *Macromolecules* **2010**, *43*, 6234.

(15) Ramani, R.; Valkama, S.; Kilpelainen, S.; Tumisto, F.; ten Brinke, G.; Ruokolainen, J.; Alam, S.; Ikkala, O. *Phys. Status Solidi C: Curr. Top. Solid State Phys.* **2009**, *6*, 2414.
(16) Jiang, Z. B.; Wang, R.; Xue, G. *J. Phys. Chem. B* **2009**, *113*, 7462.
(17) Kumar, R.; Muthukumar, M. *J. Chem. Phys.* **2007**, *126*, 214902.
(18) Lefebvre, M. D.; de la Cruz, M. O.; Shull, K. R. *Macromolecules* **2004**, *37*, 1118.
(19) Wang, Y. Q.; Li, X. A.; Tang, P.; Yang, Y. L. *Physica B-Condens. Matter* **2011**, *406*, 1132.
(20) Beardsley, T. M.; Matsen, M. W. *Eur. Phys. J. E* **2008**, *27*, 323.
(21) Sides, S. W.; Fredrickson, G. H. *J. Chem. Phys.* **2004**, *121*, 4974.
(22) Cooke, D. M.; Shi, A.-C. *Macromolecules* **2006**, *39*, 6661.
(23) Drolet, F.; Fredrickson, G. H. *Phys. Rev. Lett.* **1999**, *83*, 4317.
(24) Drolet, F.; Fredrickson, G. H. *Macromolecules* **2001**, *34*, 5317.
(25) Bohbot-Raviv, Y.; Wang, Z. G. *Phys. Rev. Lett.* **2000**, *85*, 3428.
(26) Wang, R.; Jiang, Z. B.; Hu, J. L. *Polymer* **2005**, *46*, 6201.
(27) Khalatur, P. G.; Khokhlov, A. R. *J. Chem. Phys.* **2000**, *112*, 4849.
(28) Shinozaki, A.; Jasnow, D.; Balazs, A. C. *Macromolecules* **1994**, *27*, 2496.
(29) Zhang, L. S.; Lin, J. P.; Lin, S. L. *J. Phys. Chem. B* **2008**, *112*, 9720.